Research Highlights

Arterial spin labeling perfusion magnetic resonance imaging of non-human primates

Xiaodong Zhang[1,2], Chun-Xia Li[1]

[1]Yerkes Imaging Center, Yerkes National Primate Research Center, Emory University, Atlanta, GA 30329, USA; [2]Division of Neuropharmacology and Neurologic Diseases, Yerkes National Primate Research Center, Emory University, Atlanta, GA, 30329, USA

Correspondence to: Xiaodong Zhang, PhD. Yerkes Imaging Center, Yerkes National Primate Research Center, Emory University, 954 Gatewood Rd NE, Atlanta, GA 30329, USA. Email: xzhang8@emory.edu.

Abstract: Non-human primates (NHPs) resemble most aspects of humans in brain physiology and anatomy and are excellent animal models for translational research in neuroscience, biomedical research and pharmaceutical development. Cerebral blood flow (CBF) offers essential physiological information of the brain to examine the abnormal functionality in NHP models with cerebral vascular diseases and neurological disorders or dementia. Arterial spin labeling (ASL) perfusion MRI techniques allow for high temporal and spatial CBF measurement and are intensively used in studies of animals and humans. In this article, current high-resolution ASL perfusion MRI techniques for quantitative evaluation of brain physiology and function in NHPs are described and their applications and limitation are discussed as well.

Keywords: Continuous arterial spin labeling (CASL); pseudo-continuous arterial spin labeling (pCASL); macaque monkey; cerebral blood flow (CBF); clinical scanner

Submitted Aug 22, 2016. Accepted for publication Sep 20, 2016.
doi: 10.21037/qims.2016.10.05
View this article at: http://dx.doi.org/10.21037/qims.2016.10.05

Introduction

Cerebral blood flow (CBF) provides critical information of brain physiology in preclinical and clinical studies. CBF can be measured quantitatively by using Xenon-133, PET, and MRI, or qualitatively with single photon emission computed tomography (SPECT), laser Doppler flowmetry (1). Arterial spin labeling (ASL) (2-7) and dynamic susceptibility contrast MRI (DSC-MRI) (8,9) techniques are the most common perfusion MRI approaches for quantitative CBF measurement with high temporal and/or spatial resolution. Perfusion MRI has been routinely used in preclinical and clinical studies of various neurological diseases like stroke (10,11). In addition, CBF-based functional MRI (fMRI) is spatially more specific to the neural activity site and has less inter-subject variation than the blood-oxygenation-level-dependent (BOLD) fMRI (12-15).

Non-human primates (NHPs) resemble most aspects of humans in brain physiology and anatomy in comparison with other animal species and are excellent animal models in neuroscience, biomedical and pharmaceutical research, and vaccine development (16-18). Both DSC-MRI and ASL perfusion MRI techniques have been developed to examine the functionality and physiological conditions in the NHP brain. In comparison with DSC-MRI, ASL uses magnetically labelling endogenous water in the arterial blood as freely diffusible tracer and does not require the administration of contrast agents. Therefore it is a completely non-invasive MRI technique. In particular, as the labeled water has a short half-life (~blood T_1), ASL-based perfusion MRI can be repeatedly conducted to detect the temporal homodynamic changes in the brain with/without task activation or quantitatively measure basal or resting CBF with high spatial resolution. In this article, current ASL-based perfusion MRI techniques are described and their application and limitations in NHP studies are discussed as well.

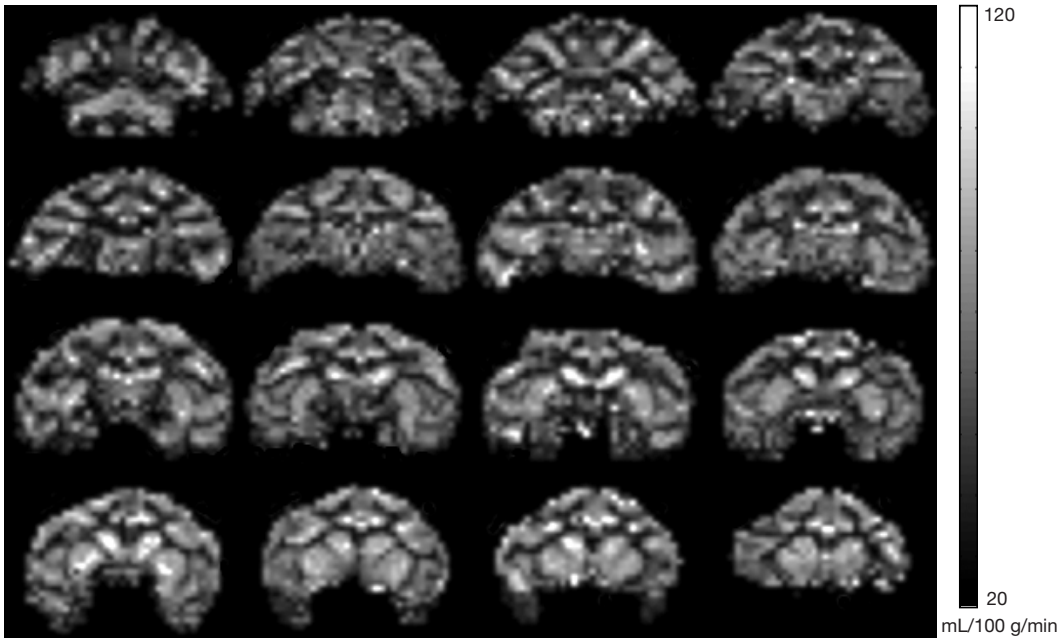

Figure 1 Coronal CBF maps of an adult macaque monkey acquired using a 3-coil continuous ASL technique on a clinical 3T scanner. Voxel size: 1.5×1.5×1.5 mm^3. Acquisition time: 3 minutes [Reprinted with permission (28)]. CBF, cerebral blood flow; ASL, arterial spin labeling.

ASL perfusion MRI techniques

ASL perfusion MRI is usually achieved with the continuous arterial spin labeling (CASL) technique (3,19-21) in which a separate neck coil is placed under the neck for labeling the arterial blood water. It can also be conducted using pulsed arterial spin labeling (PASL) (2,4,5), amplitude-modulated CASL technique (22), pseudo-continuous arterial spin labeling (pCASL) technique (23), in which the blood water labelling and brain imaging are implemented using the same imaging coil. Compared to PASL, CASL allows for continuous supply of labeled arterial blood water into tissue of interest, offering greater detection sensitivity and large volume coverage for CBF measurement. Current CASL techniques for NHP studies are described and discussed below.

CASL perfusion MRI with a separate labeling coil

Compared to regular single-coil ASL techniques, CASL with a separate labeling coil uses a long RF pulse (up to couple seconds) to adiabatically invert the flowing spins in the arterial blood locally (normally in the neck area where the labeling coil is placed). Therefore, it has greater signal to noise ratio (SNR) and reduced specific absorption rate (SAR), particularly in small animals (like rodents) which have short arterial transit time (ATT) (24,25). Also, magnetization-transfer (MT) effect can be eliminated when the RF transmission, imaging, and labeling coils are properly decoupled with each other (26). Such CASL technique is usually available on research scanners for small animals and dedicated research scanners for NHPs (27). A few conventional clinical scanners have been developed for CBF measurement with a separate labeling coil in humans (19,20) and NHPs (28,29). In the three-coil ASL setting (28), a receive-only surface coil is used for imaging, allowing for maximal sensitivity in measuring CBF of the macaque monkey brain (*Figure 1*). This novel setting has particular advantage to examine the local hemodynamic changes of the cortex in fMRI studies of NHPs (27). However, the CBF maps may be biased in deep brain regions due to the inherent SNR heterogeneity of a surface coil. In addition, it is not an ideal setting for multi-parameter MRI of the whole brain as some MRI modalities like diffusion tensor imaging (DTI) or diffusion spectrum imaging (DSI) are susceptible to the inhomogeneous sensitivity of a surface coil and novel parallel imaging and multiband MRI techniques cannot be performed due to the lack of multiple channels. In contrast, a two-coil setting in which a transmit/receive phased-array

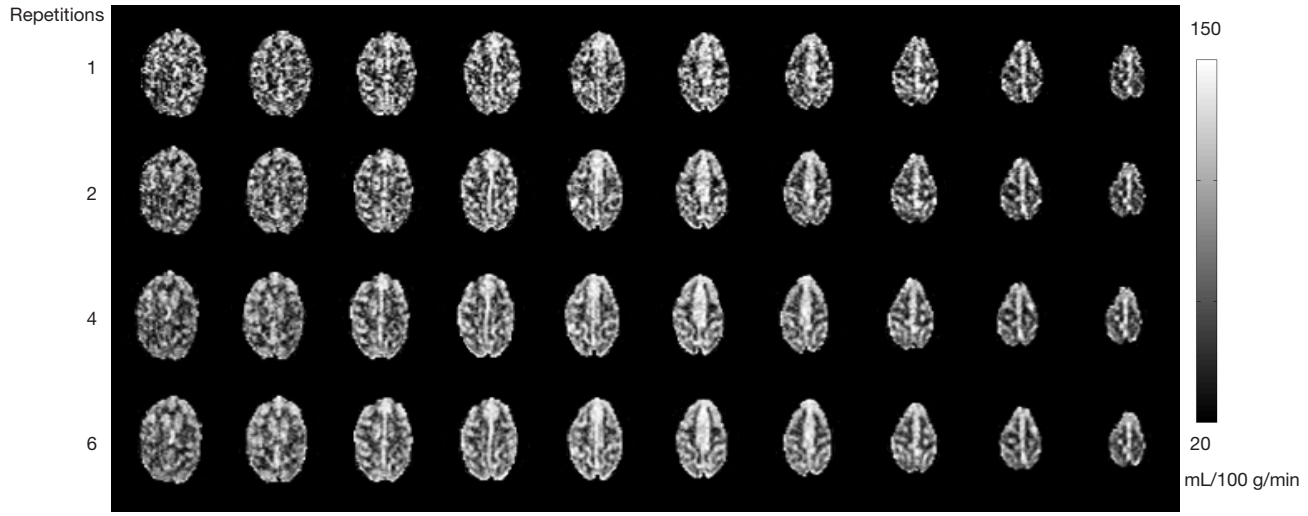

Figure 2 Axial CBF maps of an adult macaque monkey averaged with different repetitions using a 2-coil CASL setting on a clinical 3T scanner. Voxel size: 1.5×1.5×1.5 mm^3. Acquisition time for one repetition: 5 minutes. CBF, cerebral blood flow; CASL, continuous arterial spin labeling.

volume coil is employed for imaging can be used to collect homogeneous CBF maps with the tradeoff of reduced SNR (*Figure 2*), allowing for multi-parameter MRI measures of the whole brain performed in a single scanning session. In particular, many MRI modalities using novel parallel imaging and multiband MRI techniques can be explored in NHP studies on such two-coil setting (30-34). The repetition effect of ASL data acquisition is illustrated also (*Figure 2*). Our experiences suggest 4–6 repetitions of ASL data acquisition (each repetition lasts 5 minutes) provide suitable CBF maps of anesthetized macaque monkeys, and longer data acquisition does not substantially improve the quality of CBF maps by image averaging.

CASL perfusion MRI with a single coil

The ASL technique with a separate labeling coil is an ideal setting for CBF measurements of NHPs using a research or conventional clinic scanner (27-29). However, such CASL technique is not accessible in most clinical scanners as it requires additional RF hardware and software. In contrast, the pCASL MRI technique allows for using the same RF coil for labeling and imaging. Accordingly CBF measurement can be carried out without installing additional hardware on the scanner (35-38). With pCASL, the continuous labeling of the spins in the arterial blood water is implemented by using a train of rapid repeating short RF pulses (usually <1 ms) with alternating sign magnetic field gradients to mimic the spin-labeling scheme in CASL with a separate labeling coil. To date, pCASL technique has been implemented by most scanner manufactures, providing a robust and convenient means to measure CBF of NHPs using a standard clinical setting (*Figure 3*). As expected, the SNR of the CBF maps is reduced compared to those acquired with a separate labeling coil (*Figures 1,2*). Multi-parameter MRI with parallel imaging techniques allows for multiple MRI parameters to be measured from one subject within a single scanning session and is becoming an effective tool to characterize the tissue injury and function recovery in stroke and other diseases (31,40,41). Therefore, such single-coil setting allows for pCASL-based perfusion MRI to be conducted together with other modalities such as T_1, T_2-weighted, spectroscopy, fMRI, DTI on a standard clinical scanner. Among the single coil ASL techniques, amplitude-modulated CASL techniques (22) and pCASL techniques (36,42) have been successfully implemented for brain perfusion studies in macaque models of neuro-AIDS (43) and healthy adult macaque monkeys (39).

CBF quantification

Multiple numerical models have been developed for CBF quantification (44). Single-compartment (6,45,46) is a simplified but popular model in which water is assumed to be a freely diffusible tracer and the exchange of the tracer with the tissue water is instantaneous. In contrast, some

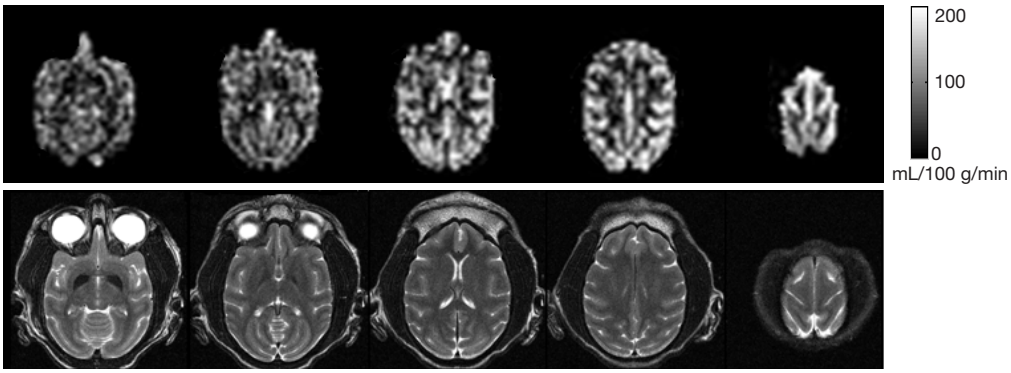

Figure 3 Axial CBF maps (top) and T2-weighted anatomical images of an adult macaque monkey acquired using pCASL technique on a clinical 3T scanner. Voxel size: 1.5 ×1.5×1.5mm^3. Six averages. Acquisition time for one repetition: 5 minutes [Reprinted with permission (39)]. CBF, cerebral blood flow; pCASL, pseudo-continuous arterial spin labeling.

two-compartment models take into account of the effects of capillary wall permeability for restricted water exchange (47-49).

The regional difference in ATT is usually not considered in simplified CBF calculation (50), or a single ATT value in grey matter (GM) is used for the entire brain CBF calculation (28). Prior studies suggest that ASL-based CBF is sensitive to the changes of ATT (45,51,52). It has been suggested that ATT needs to be taken into account to obtain quantitatively accurate CBF maps (53,54). In particular, the perfusion quantification in white matter (WM) can be strongly biased as the ATT of WM is longer than that in GM (55). Since rodents have little WM, using a fixed ATT value may not cause significant error in CBF quantification of rodents. However, it may introduce severe bias in quantification of WM CBF in NHP or human brains as the WM can fill up to ~60 percent of the brain.

The model proposed by Alsop and colleagues considers the contribution from the tissue compartment and vascular compartment (45,56). With this model, CBF and ATT maps can be estimated pixel by pixel from CASL measurements with different post-labeling delays. The CBF calculation with this formula requires multi-parameter non-linear curve fitting. Because of the lack of the prior knowledge about these parameters and the low SNR of ASL signals during the fitting procedure, the CBF and ATT maps can be severely biased. The multiresolution data analysis approach has been demonstrated previously to improve quantification of *in vivo* MR spectroscopy and MRI (57-59). Briefly, the multiresolution strategy consists of constructing a multiresolution pyramid dataset of re-sampled spatial resolution from coarse to fine in which the coarse dataset has smaller data matrix but improved SNR in each pixel due to the average effect across the corresponding neighbor pixels in the finer level. Therefore, the initial fitting parameters are estimated firstly by fitting the dataset on the top of pyramid in which the data has highest SNR. Then these parameters are used as prior knowledge for fitting the data set at the next finer resolution. This procedure is repeated until the original resolution is reached. The multiresolution or multiscale processing strategy has been explored for CBF and ATT estimation as reported in our preliminary study (60), in which CBF and ATT maps were derived using the numerical model for CBF quantification (56) and a modified equation for the elimination of magnetization transfer effect using a separate labeling coil is utilized as shown in Eq. [1]:

$$\Delta M = \frac{2\alpha M_b^0 f}{\lambda}\left\{T_{1tis} * exp(\frac{-\delta}{T_{1\alpha}}) * exp(\frac{min(\delta - w, 0)}{T_{1tis}}) + T_{1\alpha}\left[exp(\frac{min(\delta_\alpha - w, 0) - \delta_\alpha}{T_{1\alpha}}) - exp(\frac{min(\delta - w, 0) - \delta}{T_{1\alpha}})\right]\right\} \quad [1]$$

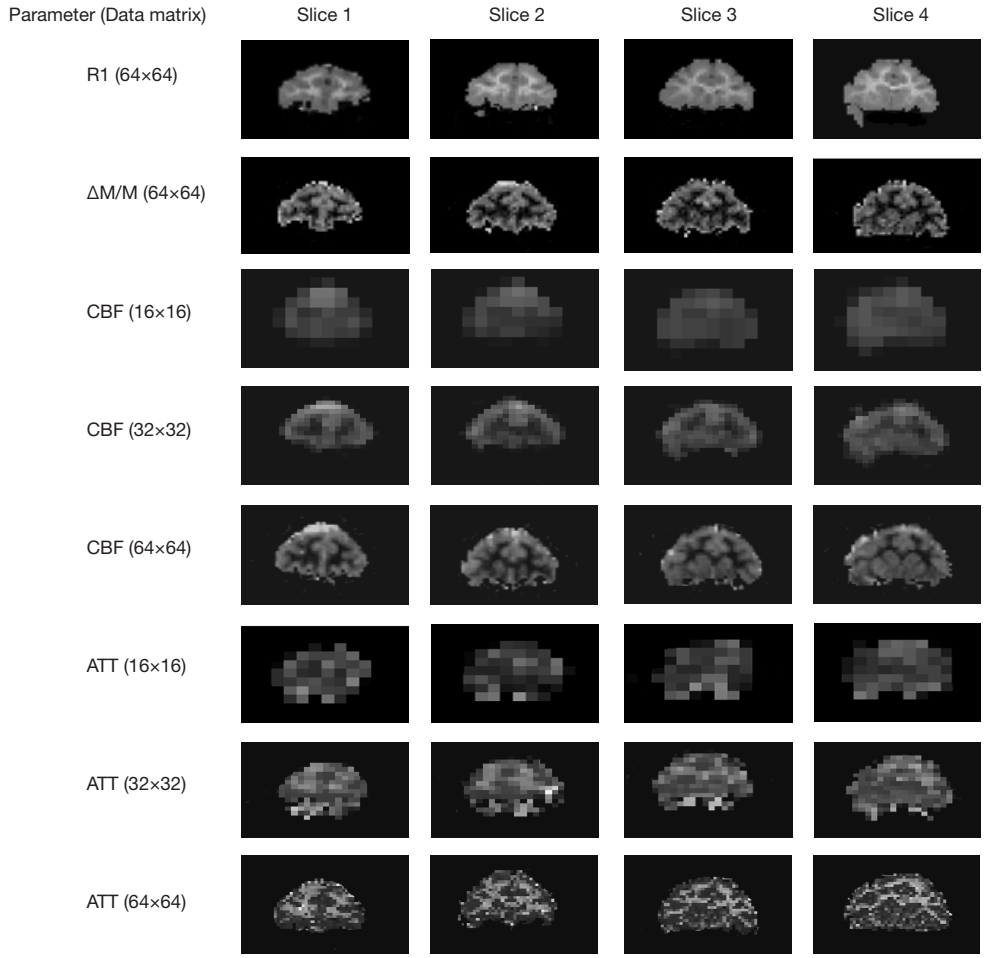

Figure 4 Coronal CBF and ATT maps of an adult macaque monkey calculated with a multiscale approach. Voxel size: 1.5×1.5×1.5 mm^3. R1: relaxation rate ($1/T_1$). ΔM/M: raw EPI image intensity change ratio with ASL. CBF, cerebral blood flow; ATT, arterial transit time; ASL, arterial spin labeling; EPI, echo-planar imaging.

In which M_b^0 is the equilibrium magnetization, α is the labeling efficiency, f is the CBF in mL/g/s. λ is the brain-blood partition coefficient, T_{1tis} is the tissue T_1, and T_{1a} is the blood T_1. δ_a (or ATT) is the transit time from the labeling plane to the arterial compartment, δ is the transit time from the labeling plane to the imaging slice, w is the post-labeling-delay. λ=0.9, α=92%, T_{1a}=1.66 s at 3T, and T_1 map was obtained using an echo-planar imaging (EPI)-based inversion recovery measurement as described in the previous report (28).

The original data matrix size of the demonstrated perfusion images was 64×64 (*Figure 4*). A pyramid of three layers (from top to bottom: 16×16, 32×32, and 64×64) was constructed. The multiscale procedure was applied to generate CBF and ATT maps at each resolution level. As seen in *Figure 4*, GM shows much shorter ATT (~0.5 seconds) compared to those in WM (~0.9 seconds). The results suggest that multiresolution strategy is an efficient and robust approach for estimating multiple parameters from ASL data.

Technical challenges and limitations of ASL perfusion MRI in NHPs

To date, whole body high-field (3T) MRI clinical scanners are installed in most clinics or neuroimaging centers, greatly facilitating the use of novel MRI techniques in biomedical research using NHPs. In particular, the clinical scanners have spacious bore size which offers sufficient room for NHP handling in various experimental settings.

Also, the related MRI findings can be readily translational compared to rodent studies with ultrahigh field scanners. As the usage of NHPs in scientific procedures is highly restrained by the ethics and rationale and cost as well (all procedures are specifically guided by the NIH guidelines for animal care and use in the United States), non-invasive *in vivo* MRI techniques play a unique and important role for accessing anatomical, physiological and functional information of NHP brains (61-64). The sample size in NHP neuroimaging studies is usually much smaller than that in rodents. Each scan must be carefully performed in order to obtain optimal images and minimize inter-subject variation for greater chance to reach statistical significance in the data analysis.

CASL with a separate labeling coil (two or three coil setting) provides optimal means for detection of basal CBF or function activation in NHPs. In particular, the receiving surface coil can be adjusted properly for maximal sensitivity to detect the local hemodynamic changes in the cortex with very high spatial and temporal resolution, greatly benefiting fMRI studies. In contrast, pCASL can be performed with a standard clinic setting and is currently available in most clinical scanners, largely facilitating CBF measurement in various NHP studies. pCASL can be used independently or easily combined with other MRI modalities (like DTI, structural MRI, *in vivo* MR spectroscopy) (31,41), providing sufficient quality data of resting CBF to examine the physiology in normal or stroke NHP brains. The labeling efficiency in pCASL is susceptible to the B0 and B1 field inhomogeneity and can vary substantially from animal to animal due to the variation in animal body size, shape and the inconsistency of experimental setting and should be calibrated in each scan. In addition, simultaneous multi-slice imaging (35), background suppression and 3D gradient and spin echo (GRASE) based ASL techniques (65) can improve image coverage and quality or offer better repeatability in ASL perfusion MRI studies and should be further explored in NHP models. The advance of ultra-high MRI (7T or above) also benefits the ASL techniques for NHP studies due to increased SNR of the MR images and longer T_1 relaxation times of blood water and tissue in the brain (66).

Anesthetized animals are generally applied in MRI studies to minimize the animal motion even though MRI of awake NHPs can eliminate the adverse anesthesia effects in the brain but it requires extensive animal training and special experimental settings (67-69) which are not available in most research labs. Even though anesthetics like isoflurane substantially suppress the neural activation in the NHP brain, the brain functionality can still be evaluated with fMRI techniques (70,71). Also, the handling of anesthetized NHPs requires comprehensive physiological monitoring and professional veterinarian support to maintain animals in proper conditions and comply with the NIH guidelines of animal care and usage. The animal physiology can be altered due to adverse anesthesia effects. It is important to maintain the animal physiology in the stable condition and within normal ranges in every MRI scan in order to ensure the consistency of ASL data collection from one subject to another. The anesthesia effects can play a critical role in examining the functionality of NHPs and should be considered in experimental design and interpretation of the outcome using MRI (29,72).

Conclusions

CASL-based perfusion MRI allows for quantitative assessment of resting or dynamic CBF in NHPs using contemporary high field clinical scanners and has wide applications in NHP models with neurological diseases. Optimal CBF measurement in NHPs requires specific management on hardware and software, pulse sequences, data processing, and professional animal handling on a conventional clinical setting. With the advances of ASL perfusion techniques in high or ultra-high MRI, the further exploration of perfusion MRI techniques will advance the translational research using NHPs as animals keep playing a critical role in contemporary neuroscience and translational biomedical research and pharmaceutical development.

Acknowledgements

Funding: The project was funded by the National Center for Research Resources (P51RR000165) and is currently supported by the Office of Research Infrastructure Programs (OD P51OD011132).

Footnote

Conflicts of Interest: The authors have no conflicts of interest to declare.

References

1. Wintermark M, Sesay M, Barbier E, Borbély K, Dillon WP, Eastwood JD, Glenn TC, Grandin CB, Pedraza S,

Soustiel JF, Nariai T, Zaharchuk G, Caillé JM, Dousset V, Yonas H. Comparative overview of brain perfusion imaging techniques. Stroke 2005;36:e83-99.
2. Kim SG. Quantification of relative cerebral blood flow change by flow-sensitive alternating inversion recovery (FAIR) technique: application to functional mapping. Magn Reson Med 1995;34:293-301.
3. Silva AC, Zhang W, Williams DS, Koretsky AP. Multi-slice MRI of rat brain perfusion during amphetamine stimulation using arterial spin labeling. Magn Reson Med 1995;33:209-14.
4. Detre JA, Zhang W, Roberts DA, Silva AC, Williams DS, Grandis DJ, Koretsky AP, Leigh JS. Tissue specific perfusion imaging using arterial spin labeling. NMR Biomed 1994;7:75-82.
5. Wong EC, Buxton RB, Frank LR. Quantitative imaging of perfusion using a single subtraction (QUIPSS and QUIPSS II). Magn Reson Med 1998;39:702-8.
6. Williams DS, Detre JA, Leigh JS, Koretsky AP. Magnetic resonance imaging of perfusion using spin inversion of arterial water. Proc Natl Acad Sci U S A 1992;89:212-6.
7. Detre JA, Leigh JS, Williams DS, Koretsky AP. Perfusion imaging. Magn Reson Med 1992;23:37-45.
8. Østergaard L. Principles of cerebral perfusion imaging by bolus tracking. J Magn Reson Imaging 2005;22:710-7.
9. Belliveau JW, Kennedy DN Jr, McKinstry RC, Buchbinder BR, Weisskoff RM, Cohen MS, Vevea JM, Brady TJ, Rosen BR. Functional mapping of the human visual cortex by magnetic resonance imaging. Science 1991;254:716-9.
10. Calamante F, Thomas DL, Pell GS, Wiersma J, Turner R. Measuring cerebral blood flow using magnetic resonance imaging techniques. J Cereb Blood Flow Metab 1999;19:701-35.
11. Nael K, Kubal W. Magnetic Resonance Imaging of Acute Stroke. Magn Reson Imaging Clin N Am 2016;24:293-304.
12. Davis TL, Kwong KK, Weisskoff RM, Rosen BR. Calibrated functional MRI: mapping the dynamics of oxidative metabolism. Proc Natl Acad Sci U S A 1998;95:1834-9.
13. Kim SG, Uğurbil K. Comparison of blood oxygenation and cerebral blood flow effects in fMRI: estimation of relative oxygen consumption change. Magn Reson Med 1997;38:59-65.
14. Hoge RD, Atkinson J, Gill B, Crelier GR, Marrett S, Pike GB. Linear coupling between cerebral blood flow and oxygen consumption in activated human cortex. Proc Natl Acad Sci U S A 1999;96:9403-8.
15. Detre JA, Wang J. Technical aspects and utility of fMRI using BOLD and ASL. Clin Neurophysiol 2002;113:621-34.
16. Cook DJ, Tymianski M. Nonhuman primate models of stroke for translational neuroprotection research. Neurotherapeutics 2012;9:371-9.
17. Hutchison RM, Everling S. Monkey in the middle: why non-human primates are needed to bridge the gap in resting-state investigations. Front Neuroanat 2012;6:29.
18. Rivera-Hernandez T, Carnathan DG, Moyle PM, Toth I, West NP, Young PR, Silvestri G, Walker MJ. The contribution of non-human primate models to the development of human vaccines. Discov Med 2014;18:313-22.
19. Zaharchuk G, Ledden PJ, Kwong KK, Reese TG, Rosen BR, Wald LL. Multislice perfusion and perfusion territory imaging in humans with separate label and image coils. Magn Reson Med 1999;41:1093-8.
20. Talagala SL, Ye FQ, Ledden PJ, Chesnick S. Whole-brain 3D perfusion MRI at 3.0 T using CASL with a separate labeling coil. Magn Reson Med 2004;52:131-40.
21. Xu Q, Glielmi C, Zhou L, Choi K, Hu X. An Inexpensive and Programmable RF Transmitter Setup for Two-coil CASL. Concepts Magn Reson Part B Magn Reson Eng 2008;33B:228-35.
22. Wang J, Zhang Y, Wolf RL, Roc AC, Alsop DC, Detre JA. Amplitude-modulated continuous arterial spin-labeling 3.0-T perfusion MR imaging with a single coil: feasibility study. Radiology 2005;235:218-28.
23. Alsop DC, Detre JA, Golay X, Günther M, Hendrikse J, Hernandez-Garcia L, Lu H, MacIntosh BJ, Parkes LM, Smits M, van Osch MJ, Wang DJ, Wong EC, Zaharchuk G. Recommended implementation of arterial spin-labeled perfusion MRI for clinical applications: A consensus of the ISMRM perfusion study group and the European consortium for ASL in dementia. Magn Reson Med 2015;73:102-16.
24. Silva AC, Lee SP, Yang G, Iadecola C, Kim SG. Simultaneous blood oxygenation level-dependent and cerebral blood flow functional magnetic resonance imaging during forepaw stimulation in the rat. J Cereb Blood Flow Metab 1999;19:871-9.
25. Duong TQ, Silva AC, Lee SP, Kim SG. Functional MRI of calcium-dependent synaptic activity: cross correlation with CBF and BOLD measurements. Magn Reson Med 2000;43:383-92.
26. Zhang W, Silva AC, Williams DS, Koretsky AP. NMR measurement of perfusion using arterial spin labeling

without saturation of macromolecular spins. Magn Reson Med 1995;33:370-6.
27. Zappe AC, Pfeuffer J, Merkle H, Logothetis NK, Goense JB. The effect of labeling parameters on perfusion-based fMRI in nonhuman primates. J Cereb Blood Flow Metab 2008;28:640-52.
28. Zhang X, Nagaoka T, Auerbach EJ, Champion R, Zhou L, Hu X, Duong TQ. Quantitative basal CBF and CBF fMRI of rhesus monkeys using three-coil continuous arterial spin labeling. Neuroimage 2007;34:1074-83.
29. Li CX, Patel S, Auerbach EJ, Zhang X. Dose-dependent effect of isoflurane on regional cerebral blood flow in anesthetized macaque monkeys. Neurosci Lett 2013;541:58-62.
30. Auerbach EJ, Xu J, Yacoub E, Moeller S, Uğurbil K. Multiband accelerated spin-echo echo planar imaging with reduced peak RF power using time-shifted RF pulses. Magn Reson Med 2013;69:1261-7.
31. Zhang X, Tong F, Li CX, Yan Y, Nair G, Nagaoka T, Tanaka Y, Zola S, Howell L. A fast multiparameter MRI approach for acute stroke assessment on a 3T clinical scanner: preliminary results in a non-human primate model with transient ischemic occlusion. Quant Imaging Med Surg 2014;4:112-22.
32. Meng Y, Zhang X. In vivo diffusion spectrum imaging of non-human primate brain: initial experience in transcallosal fiber examination. Quant Imaging Med Surg 2014;4:129-35.
33. Meng Y, Zhang X. Corticospinal Tract Distribution in Motor Cortices of Adult Macaque Brains Revealed by High Angular Resolution Diffusion Imaging (HARDI) Tractography. Proceedings of the 25th Annual Meeting of ISMRM, Singapore, 2016;3478.
34. Feinberg DA, Setsompop K. Ultra-fast MRI of the human brain with simultaneous multi-slice imaging. J Magn Reson 2013;229:90-100.
35. Wang Y, Moeller S, Li X, Vu AT, Krasileva K, Ugurbil K, Yacoub E, Wang DJ. Simultaneous multi-slice Turbo-FLASH imaging with CAIPIRINHA for whole brain distortion-free pseudo-continuous arterial spin labeling at 3 and 7 T. Neuroimage 2015;113:279-88.
36. Wu WC, Fernández-Seara M, Detre JA, Wehrli FW, Wang J. A theoretical and experimental investigation of the tagging efficiency of pseudocontinuous arterial spin labeling. Magn Reson Med 2007;58:1020-7.
37. Jain V, Duda J, Avants B, Giannetta M, Xie SX, Roberts T, Detre JA, Hurt H, Wehrli FW, Wang DJ. Longitudinal reproducibility and accuracy of pseudo-continuous arterial spin-labeled perfusion MR imaging in typically developing children. Radiology 2012;263:527-36.
38. Dai W, Garcia D, de Bazelaire C, Alsop DC. Continuous flow-driven inversion for arterial spin labeling using pulsed radio frequency and gradient fields. Magn Reson Med 2008;60:1488-97.
39. Li CX, Patel S, Wang DJ, Zhang X. Effect of high dose isoflurane on cerebral blood flow in macaque monkeys. Magn Reson Imaging 2014;32:956-60.
40. Jacobs MA, Mitsias P, Soltanian-Zadeh H, Santhakumar S, Ghanei A, Hammond R, Peck DJ, Chopp M, Patel S. Multiparametric MRI tissue characterization in clinical stroke with correlation to clinical outcome: part 2. Stroke 2001;32:950-7.
41. Lauzon ML, Sevick RJ, Demchuk AM, Frayne R. Stroke imaging at 3.0 T. Neuroimaging Clin N Am 2006;16:343-66, xii.
42. Silva AC, Kim SG. Pseudo-continuous arterial spin labeling technique for measuring CBF dynamics with high temporal resolution. Magn Reson Med 1999;42:425-9.
43. Li C, Zhang X, Komery A, Li Y, Novembre FJ, Herndon JG. Longitudinal diffusion tensor imaging and perfusion MRI investigation in a macaque model of neuro-AIDS: a preliminary study. Neuroimage 2011;58:286-92.
44. Steger TR, White RA, Jackson EF. Input parameter sensitivity analysis and comparison of quantification models for continuous arterial spin labeling. Magn Reson Med 2005;53:895-903.
45. Alsop DC, Detre JA. Reduced transit-time sensitivity in noninvasive magnetic resonance imaging of human cerebral blood flow. J Cereb Blood Flow Metab 1996;16:1236-49.
46. Wong EC, Buxton RB, Frank LR. Implementation of quantitative perfusion imaging techniques for functional brain mapping using pulsed arterial spin labeling. NMR Biomed 1997;10:237-49.
47. Wu CW, Liu HL, Chen JH, Yang Y. Effects of CBV, CBF, and blood-brain barrier permeability on accuracy of PASL and VASO measurement. Magn Reson Med 2010;63:601-8.
48. Parkes LM, Tofts PS. Improved accuracy of human cerebral blood perfusion measurements using arterial spin labeling: accounting for capillary water permeability. Magn Reson Med 2002;48:27-41.
49. Zhou J, Wilson DA, Ulatowski JA, Traystman RJ, van Zijl PC. Two-compartment exchange model for perfusion quantification using arterial spin tagging. J Cereb Blood Flow Metab 2001;21:440-55.

50. Silva AC, Kim SG, Garwood M. Imaging blood flow in brain tumors using arterial spin labeling. Magn Reson Med 2000;44:169-73.
51. Wang J, Alsop DC, Li L, Listerud J, Gonzalez-At JB, Schnall MD, Detre JA. Comparison of quantitative perfusion imaging using arterial spin labeling at 1.5 and 4.0 Tesla. Magn Reson Med 2002;48:242-54.
52. Buxton RB, Frank LR, Wong EC, Siewert B, Warach S, Edelman RR. A general kinetic model for quantitative perfusion imaging with arterial spin labeling. Magn Reson Med 1998;40:383-96.
53. Frank LR, Wong EC, Buxton RB. Slice profile effects in adiabatic inversion: application to multislice perfusion imaging. Magn Reson Med 1997;38:558-64.
54. Yang Y, Engelien W, Xu S, Gu H, Silbersweig DA, Stern E. Transit time, trailing time, and cerebral blood flow during brain activation: measurement using multislice, pulsed spin-labeling perfusion imaging. Magn Reson Med 2000;44:680-5.
55. Kamba M, Suto Y, Ogawa T. Measurement of cerebral mean transit time by dynamic susceptibility contrast magnetic resonance imaging. Eur J Radiol 1999;31:170-3.
56. Gonzalez-At JB, Alsop DC, Detre JA. Cerebral perfusion and arterial transit time changes during task activation determined with continuous arterial spin labeling. Magn Reson Med 2000;43:739-46.
57. Zhang X, Heberlein K, Sarkar S, Hu X. A multiscale approach for analyzing in vivo spectroscopic imaging data. Magn Reson Med 2000;43:331-4.
58. Zhang X, Hu X. Peak-specific phase correction for automated spectrum processing of in vivo magnetic resonance spectroscopic imaging by using the multiscale approach. Bo Pu Xue Za Zhi 2014;31:32-9.
59. Lu W, Hargreaves BA. Multiresolution field map estimation using golden section search for water-fat separation. Magn Reson Med 2008;60:236-44.
60. Zhang X, Nagaoka T, Champion R, Duong T. Multiresolution strategy to estimate arterial transit time and cerebral-blood-flow maps in rhesus monkeys. Proceedings of the 16th Annual Meeting of International Society of Magnetic Resonance in Medicine (ISMRM), Berlin, 2007:1426.
61. Zhang X. Magnetic resonance imaging of non-human primate ischemic stroke models. Chinese Journal of Magnetic Resonance 2010;27:548-60.
62. Zhang X, Li C. Quantitative MRI Measures in SIV-Infected Macaque Brains. J Clin Cell Immunol 2013;Suppl 7. pii: 005.
63. Logothetis NK. MR imaging in the non-human primate: studies of function and of dynamic connectivity. Curr Opin Neurobiol 2003;13:630-42.
64. Genain CP. MR imaging investigations in a non-human primate model of multiple sclerosis. AJNR Am J Neuroradiol 1999;20:955-7.
65. Vidorreta M, Wang Z, Rodríguez I, Pastor MA, Detre JA, Fernández-Seara MA. Comparison of 2D and 3D single-shot ASL perfusion fMRI sequences. Neuroimage 2013;66:662-71.
66. Zuo Z, Wang R, Zhuo Y, Xue R, St Lawrence KS, Wang DJ. Turbo-FLASH based arterial spin labeled perfusion MRI at 7 T. PLoS One 2013;8:e66612.
67. Maltbie E, Gopinath K, Urushino N, Kempf D, Howell L. Ketamine-induced brain activation in awake female nonhuman primates: a translational functional imaging model. Psychopharmacology (Berl) 2016;233:961-72.
68. Hung CC, Yen CC, Ciuchta JL, Papoti D, Bock NA, Leopold DA, Silva AC. Functional MRI of visual responses in the awake, behaving marmoset. Neuroimage 2015;120:1-11.
69. Belcher AM, Yen CC, Stepp H, Gu H, Lu H, Yang Y, Silva AC, Stein EA. Large-scale brain networks in the awake, truly resting marmoset monkey. J Neurosci 2013;33:16796-804.
70. Meng Y, Hu X, Bachevalier J, Zhang X. Decreased functional connectivity in dorsolateral prefrontal cortical networks in adult macaques with neonatal hippocampal lesions: Relations to visual working memory deficits. Neurobiol Learn Mem 2016;134 Pt A:31-7.
71. Zhao F, Holahan MA, Houghton AK, Hargreaves R, Evelhoch JL, Winkelmann CT, Williams DS. Functional imaging of olfaction by CBV fMRI in monkeys: insight into the role of olfactory bulb in habituation. Neuroimage 2015;106:364-72.
72. Wu TL, Wang F, Anderson AW, Chen LM, Ding Z, Gore JC. Effects of anesthesia on resting state BOLD signals in white matter of non-human primates. Magn Reson Imaging 2016;34:1235-41.

Cite this article as: Zhang X, Li CX. Arterial Spin Labeling perfusion magnetic resonance imaging of non-human primates. Quant Imaging Med Surg 2016;6(5):573-581. doi: 10.21037/qims.2016.10.05

